Privacy-Preserving and Truthful Detection of Packet Dropping Attacks in Wireless Ad Hoc Networks

Tao Shu and Marwan Krunz, *Fellow, IEEE*

Abstract—Link error and malicious packet dropping are two sources for packet losses in multi-hop wireless ad hoc network. In this paper, while observing a sequence of packet losses in the network, we are interested in determining whether the losses are caused by link errors only, or by the combined effect of link errors and malicious drop. We are especially interested in the insider-attack case, whereby malicious nodes that are part of the route exploit their knowledge of the communication context to selectively drop a small amount of packets critical to the network performance. Because the packet dropping rate in this case is comparable to the channel error rate, conventional algorithms that are based on detecting the packet loss rate cannot achieve satisfactory detection accuracy. To improve the detection accuracy, we propose to exploit the correlations between lost packets. Furthermore, to ensure truthful calculation of these correlations, we develop a homomorphic linear authenticator (HLA) based public auditing architecture that allows the detector to verify the truthfulness of the packet loss information reported by nodes. This construction is privacy preserving, collusion proof, and incurs low communication and storage overheads. To reduce the computation overhead of the baseline scheme, a packet-block-based mechanism is also proposed, which allows one to trade detection accuracy for lower computation complexity. Through extensive simulations, we verify that the proposed mechanisms achieve significantly better detection accuracy than conventional methods such as a maximum-likelihood based detection.

Index Terms—Packet dropping, secure routing, attack detection, homomorphic linear signature, auditing

1 Introduction

In a multi-hop wireless network, nodes cooperate in relaying/routing traffic. An adversary can exploit this cooperative nature to launch attacks. For example, the adversary may first pretend to be a cooperative node in the route discovery process. Once being included in a route, the adversary starts dropping packets. In the most severe form, the malicious node simply stops forwarding every packet received from upstream nodes, completely disrupting the path between the source and the destination. Eventually, such a severe denial-of-service (DoS) attack can paralyze the network by partitioning its topology.

Even though persistent packet dropping can effectively degrade the performance of the network, from the attacker's standpoint such an "always-on" attack has its disadvantages. First, the continuous presence of extremely high packet loss rate at the malicious nodes makes this type of attack easy to be detected [25]. Second, once being detected, these attacks are easy to mitigate. For example, in case the attack is detected but the malicious nodes are not identified, one can use the randomized multi-path routing algorithms [28], [29] to circumvent the black holes generated by the attack, probabilistically eliminating the attacker's threat. If the malicious nodes are also identified, their threats can be completely eliminated by simply deleting these nodes from the network's routing table.

A malicious node that is part of the route can exploit its knowledge of the network protocol and the communication context to launch an *insider attack*—an attack that is intermittent, but can achieve the same performance degradation effect as a persistent attack at a much lower risk of being detected. Specifically, the malicious node may evaluate the importance of various packets, and then drop the small amount that are deemed highly critical to the operation of the network. For example, in a frequency-hopping network, these could be the packets that convey frequency hopping sequences for network-wide frequency-hopping synchronization; in an ad hoc cognitive radio network, they could be the packets that carry the idle channel lists (i.e., white spaces) that are used to establish a network-wide control channel. By targeting these highly critical packets, the authors in [21], [24], [25] have shown that an intermittent insider attacker can cause significant damage to the network with low probability of being caught. In this paper, we are interested in combating such an insider attack. In particular, we are interested in the problem of detecting the occurrence of selective packet drops and identifying the malicious node(s) responsible for these drops.

Detecting selective packet-dropping attacks is extremely challenging in a highly dynamic wireless environment. The difficulty comes from the requirement that we need to not only detect the place (or hop) where the packet is dropped, but also identify whether the drop is intentional or unintentional. Specifically, due to the open nature of wireless medium, a packet drop in the network could be caused by harsh channel conditions (e.g., fading, noise, and interference, a.k.a., link errors), or by the insider attacker. In an open

• *T. Shu is with the Department of Computer Science and Engineering, Oakland University, Rochester, MI. E-mail: shu@oakland.edu.*
• *M. Krunz is with the Department of Electrical and Computer Engineering, the University of Arizona, Tucson, AZ. E-mail: krunz@email.arizona.edu.*

Manuscript received 13 Apr. 2013; revised 18 Mar. 2014; accepted 3 June 2014. Date of publication 12 June 2014; date of current version 2 Mar. 2015. For information on obtaining reprints of this article, please send e-mail to: reprints@ieee.org, and reference the Digital Object Identifier below. Digital Object Identifier no. 10.1109/TMC.2014.2330818

wireless environment, link errors are quite significant, and may not be significantly smaller than the packet dropping rate of the insider attacker. So, the insider attacker can camouflage under the background of harsh channel conditions. In this case, just by observing the packet loss rate is not enough to accurately identify the exact cause of a packet loss.

The above problem has not been well addressed in the literature. As discussed in Section 2, most of the related works preclude the ambiguity of the environment by assuming that malicious dropping is the only source of packet loss, so that there is no need to account for the impact of link errors. On the other hand, for the small number of works that differentiate between link errors and malicious packet drops, their detection algorithms usually require the number of maliciously-dropped packets to be significantly higher than link errors, in order to achieve an acceptable detection accuracy.

In this paper, we develop an accurate algorithm for detecting selective packet drops made by insider attackers. Our algorithm also provides a truthful and publicly verifiable decision statistics as a proof to support the detection decision. The high detection accuracy is achieved by exploiting the correlations between the positions of lost packets, as calculated from the auto-correlation function (ACF) of the packet-loss bitmap—a bitmap describing the lost/received status of each packet in a sequence of consecutive packet transmissions. The basic idea behind this method is that even though malicious dropping may result in a packet loss rate that is comparable to normal channel losses, the stochastic processes that characterize the two phenomena exhibit different correlation structures (equivalently, different patterns of packet losses). Therefore, by detecting the correlations between lost packets, one can decide whether the packet loss is purely due to regular link errors, or is a combined effect of link error and malicious drop. Our algorithm takes into account the cross-statistics between lost packets to make a more informative decision, and thus is in sharp contrast to the conventional methods that rely only on the distribution of the number of lost packets.

The main challenge in our mechanism lies in how to guarantee that the packet-loss bitmaps reported by individual nodes along the route are truthful, i.e., reflect the actual status of each packet transmission. Such truthfulness is essential for correct calculation of the correlation between lost packets. This challenge is not trivial, because it is natural for an attacker to report false information to the detection algorithm to avoid being detected. For example, the malicious node may understate its packet-loss bitmap, i.e., some packets may have been dropped by the node but the node reports that these packets have been forwarded. Therefore, some auditing mechanism is needed to verify the truthfulness of the reported information. Considering that a typical wireless device is resource-constrained, we also require that a user should be able to delegate the burden of auditing and detection to some public server to save its own resources.

Our solution to the above public-auditing problem is constructed based on the homomorphic linear authenticator (HLA) cryptographic primitive [2], [3], [27], which is basically a signature scheme widely used in cloud computing and storage server systems to provide a proof of storage from the server to entrusting clients [30]. However, direct application of HLA does not solve our problem well, mainly because in our problem setup, there can be more than one malicious node along the route. These nodes may collude (by exchanging information) during the attack and when being asked to submit their reports. For example, a packet and its associated HLA signature may be dropped at an upstream malicious node, so a downstream malicious node does not receive this packet and the HLA signature from the route. However, this downstream attacker can still open a back-channel to request this information from the upstream malicious node. When being audited, the downstream malicious node can still provide valid proof for the reception of the packet. So packet dropping at the upstream malicious node is not detected. Such collusion is unique to our problem, because in the cloud computing/storage server scenario, a file is uniquely stored at a single server, so there are no other parties for the server to collude with. We show that our new HLA construction is collusion-proof.

Our construction also provides the following new features. First, *privacy-preserving*: the public auditor should not be able to decern the content of a packet delivered on the route through the auditing information submitted by individual hops, no matter how many independent reports of the auditing information are submitted to the auditor. Second, our construction incurs low communication and storage overheads at intermediate nodes. This makes our mechanism applicable to a wide range of wireless devices, including low-cost wireless sensors that have very limited bandwidth and memory capacities. This is also in sharp contrast to the typical storage-server scenario, where bandwidth/storage is not considered an issue. Last, to significantly reduce the computation overhead of the baseline constructions so that they can be used in computation-constrained mobile devices, a packet-block-based algorithm is proposed to achieves scalable signature generation and detection. This mechanism allows one to trade detection accuracy for lower computation complexity.

The remainder of this paper is organized as follows. In Section 2 we review the related work. The system/adversary models and problem statement are described in Section 3. We present the proposed scheme and analyze its security performance and overheads in Section 4. The low-computation-overhead block-based algorithm is proposed in Section 5. Simulation results are presented in Section 6, and we conclude the paper in Section 7.

2 Related Work

Depending on how much weight a detection algorithm gives to link errors relative to malicious packet drops, the related work can be classified into the following two categories.

The first category aims at high malicious dropping rates, where most (or all) lost packets are caused by malicious dropping. In this case, the impact of link errors is ignored. Most related work falls into this category. Based on the methodology used to identify the attacking nodes, these works can be further classified into four sub-categories. The first sub-category is based on credit systems [9], [34], [10]. A credit system provides an incentive for cooperation. A node receives credit by relaying packets for others, and uses its credit to send its own packets. As a result, a maliciously node that continuous to drop packets will eventually deplete its credit, and will not be able to send its own traffic. The second sub-category is based on reputation systems [12], [8], [14], [19], [20], [11], [4]. A reputation system relies on neighbors to monitor and identify misbehaving nodes. A node with a high packet dropping rate is given a bad reputation by its neighbors. This reputation information is propagated periodically throughout the network and is used as an important metric in selecting routes. Consequently, a malicious node will be excluded from any route. The third sub-category of works relies on end-to-end or hop-to-hop acknowledgements to directly locate the hops where packets are lost [18], [22], [23], [5], [6], [32]. A hop of high packet loss rate will be excluded from the route. The fourth sub-category addresses the problem using cryptographic methods. For example, the work in [17] utilizes Bloom filters to construct proofs for the forwarding of packets at each node. By examining the relayed packets at successive hops along a route, one can identify suspicious hops that exhibit high packet loss rates. Similarly, the method in [16], [33] traces the forwarding records of a particular packet at each intermediate node by formulating the tracing problem as a Renyi-Ulam game. The first hop where the packet is no longer forwarded is considered a suspect for misbehaving.

The second category targets the scenario where the number of maliciously dropped packets is significantly higher than that caused by link errors, but the impact of link errors is non-negligible. Certain knowledge of the wireless channel is necessary in this case. The authors in [26] proposed to shape the traffic at the MAC layer of the source node according to a certain statistical distribution, so that intermediate nodes are able to estimate the rate of received traffic by sampling the packet arrival times. By comparing the source traffic rate with the estimated received rate, the detection algorithm decides whether the discrepancy in rates, if any, is within a reasonable range such that the difference can be considered as being caused by normal channel impairments only, or caused by malicious dropping, otherwise. The works in [13] and [31] proposed to detect malicious packet dropping by counting the number of lost packets. If the number of lost packets is significantly larger than the expected packet loss rate made by link errors, then with high probability a malicious node is contributing to packet losses.

All methods mentioned above do not perform well when malicious packet dropping is highly selective. More specifically, for the credit-system-based method, a malicious node may still receive enough credits by forwarding most of the packets it receives from upstream nodes. Similarly, in the reputation-based approach, the malicious node can maintain a reasonably good reputation by forwarding most of the packets to the next hop. While the Bloom-filter scheme is able to provide a packet forwarding proof, the correctness of the proof is probabilistic and it may contain errors. For highly selectively attacks (low packet-dropping rate), the intrinsic error rate of Bloom filer significantly undermines its detection accuracy. As for the acknowledgement-based method and all the mechanisms in the second category, merely counting the number of lost packets does not give a sufficient ground to detect the real culprit that is causing

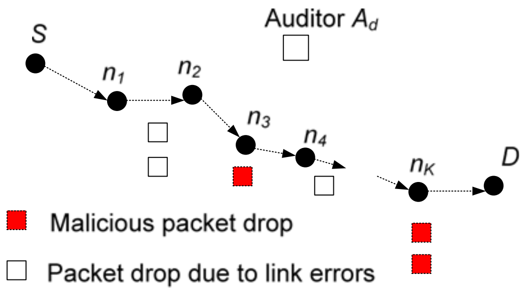

Fig. 1. Network and attack model.

packet losses. This is because the difference in the number of lost packets between the link-error-only case and the link-error-plus-malicious-dropping case is small when the attacker drops only a few packets. Consequently, the detection accuracy of these algorithms deteriorates when malicious drops become highly selective.

Our study targets the challenging situation where link errors and malicious dropping lead to comparable packet loss rates. The effort in the literature on this problem has been quite preliminary, and there is a few related works. Note that the cryptographic methods proposed in [24] to counter selective packet jamming target a different issue than the detection problem studied in this paper. The methods in [24] delay a jammer from recognizing the significance of a packet after the packet has been successfully transmitted, so that there is no time for the jammer to conduct jamming based on the content/importance of the packet. Instead of trying to detect any malicious behavior, the approach in [24] is proactive, and hence incurs overheads regardless of the presence or absence of attackers.

3 System Models and Problem Statement

3.1 Network and Channel Models

Consider an arbitrary path P_{SD} in a multi-hop wireless ad hoc network, as shown in Fig. 1. The source node S continuously sends packets to the destination node D through intermediate nodes $n_1, \ldots, n_K$, where n_i is the upstream node of n_{i+1}, for $1 \leq i \leq K-1$. We assume that S is aware of the route P_{SD}, as in Dynamic Source Routing (DSR) [15]. If DSR is not used, S can identify the nodes in P_{SD} by performing a traceroute operation. Here we mainly focus on static or quasi-static wireless ad hoc networks, i.e., we assume that the network topology and link characteristics remain unchanged for a relatively long period of time. Example networks include wireless mesh networks (WMNs) and ad hoc networks formed in nomadic computing. Extension to a highly mobile environment is out of our scope and will be considered in the future work.

We model the wireless channel of each hop along P_{SD} as a random process that alternates between good and bad states. Packets transmitted during the good state are successful, and packets transmitted during the bad state are lost. In contrast to the classical Gilbert-Ellioit (GE) channel model, here we do not assume any Markovian property on the channel behavior. We only require that the sequence of sojourn times for each state follows a stationary distribution, and the autocorrelation function of the channel state, say $f_c(i)$, where i is the time lag in packets, is also stationary. Here we limit our study to quasi-static networks, whereby the path P_{SD} remains unchanged for a relatively long time, so that the link error statistics of the wireless channel is a wide-sense stationary (WSS) random process (i.e., $f_c(i)$ is stationary). Detecting malicious packet drops may not be a concern for highly mobile networks, because the fast-changing topology of such networks makes route disruption the dominant cause for packet losses. In this case, maintaining stable connectivity between nodes is a greater concern than detecting malicious nodes. The function $f_c(i)$ can be calculated using the probing approach in [1]. In brief, a sequence of M packets are transmitted consecutively over the channel. By observing whether the transmissions are successful or not, the receiver obtains a realization of the channel state $(a_1, \ldots, a_M)$, where $a_j \in \{0, 1\}$ for $j = 1, \ldots, M$. In this sequence, "1" denotes the packet was successfully received, and "0" denotes the packet was dropped. $f_c(i)$ is derived by computing the autocorrelation function of this sample sequence: $f_c(i) \overset{\text{def}}{=} E\{a_j a_{j+i}\}$ for $i = 0, \ldots, M$, where the expectation is calculated over all transmitted packets $j = 1, \ldots, M$. This autocorrelation function describes the correlation between packet transmissions (successful/lost) at different times, as a function of the time lag. The time invariant nature of f_c is guaranteed by the WSS assumption of the wireless channel. The measurement of $f_c(i)$ can take place online or offline. A detailed discussion on how $f_c(i)$ is derived is out of the scope of this paper, and we simply assume that this information is given as input to our detection algorithm.

There is an independent auditor A_d in the network. A_d is independent in the sense that it is not associated with any node in P_{SD} and does not have any knowledge of the secrets (e.g., cryptographic keys) held by various nodes. The auditor is responsible for detecting malicious nodes on demand. Specifically, we assume S receives feedback from D when D suspects that the route is under attack. Such a suspicion may be triggered by observing any abnormal events, e.g., a significant performance drop, the loss of multiple packets of a certain type, etc. We assume that the integrity and authenticity of the feedback from D to S can be verified by S using resource-efficient cryptographic methods such as the Elliptic Curve Digital Signature Algorithm (ECDSA). Once being notified of possible attacks, S submits an *attack-detection request* (ADR) to A_d. To facilitate its investigation, A_d needs to collect certain information (elaborated on in the next section) from the nodes on route P_{SD}. We assume that each such node must reply to A_d's inquiry, otherwise the node will be considered as misbehaving. We assume that normal nodes will reply with truthful information, but malicious nodes may cheat. At the same time, for privacy reasons, we require that A_d cannot determine the content of the normal packets delivered over P_{SD} from the information collected during the auditing.

3.2 Adversarial Model

The goal of the adversary is to degrade the network's performance by maliciously dropping packets while remaining undetected. We assume that the malicious node has knowledge of the wireless channel, and is aware of the algorithm used for misbehavior detection. It has the freedom to choose what packets to drop. For example, in the random-drop mode, the malicious node may drop any packet with a small probability p_d. In the selective-mode, the malicious node only drops packets of certain types. A combination of the two modes may be used. We assume that any node on P_{SD} can be a malicious node, except the source and the destination. In particular, there can be multiple malicious nodes on P_{SD}.

We consider the following form of collusion between malicious nodes: A covert communication channel may exist between any two malicious nodes, in addition to the path connecting them on P_{SD}. As a result, malicious nodes can exchange any information without being detected by A_d or any other nodes in P_{SD}. Malicious nodes can take advantage of this covert channel to hide their misbehavior and reduce the chance of being detected. For example, an upstream malicious node may drop a packet on P_{SD}, but may secretely send this packet to a downstream malicious node via the covert channel. When being investigated, the downstream malicious node can provide a proof of the successful reception of the packet. This makes the auditor believe that the packet was successfully forwarded to the downstream nodes, and not know that the packet was actually dropped by an upstream attacker.

3.3 Problem Statement

Under the system and adversary models defined above, we address the problem of identifying the nodes on P_{SD} that drop packets maliciously. We require the detection to be performed by a public auditor that does not have knowledge of the secrets held by the nodes on P_{SD}. When a malicious node is identified, the auditor should be able to construct a publicly verifiable proof of the misbehavior of that node. The construction of such a proof should be privacy preserving, i.e., it does not reveal the original information that is transmitted on P_{SD}. In addition, the detection mechanism should incur low communication and storage overheads, so that it can be applied to a wide variety of wireless networks.

4 Proposed Detection Scheme

4.1 Overview

The proposed mechanism is based on detecting the correlations between the lost packets over each hop of the path. The basic idea is to model the packet loss process of a hop as a random process alternating between 0 (loss) and 1 (no loss). Specifically, consider that a sequence of M packets that are transmitted consecutively over a wireless channel. By observing whether the transmissions are successful or not, the receiver of the hop obtains a bitmap $(a_1, \ldots, a_M)$, where $a_j \in \{0, 1\}$ for packets $j = 1, \ldots, M$. The correlation of the lost packet is calculated as the auto-correlation function of this bitmap. Under different packet dropping conditions, i.e., link-error versus malicious dropping, the instantiations of the packet-loss random process should present distinct dropping patterns (represented by the correlation of the instance). This is true even when the packet loss rate is similar in each instantiation. To verify this property, in Fig. 2 we have simulated the auto-correlation functions of two packet loss processes, one caused by 10 percent link errors, and the other by 10 percent link errors plus 10 percent malicious uniformly-random packet dropping. It

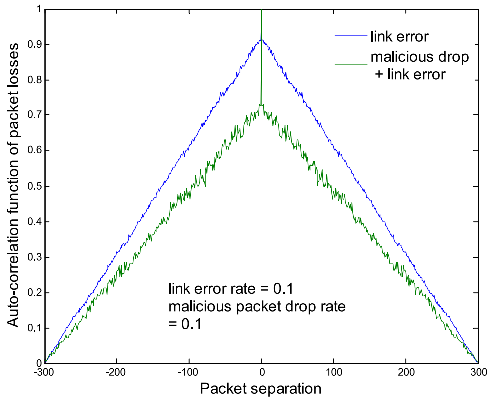

Fig. 2. Comparison of correlation of lost packets.

can be observed that significant gap exists between these two auto-correlation functions. Therefore, by comparing the auto-correlation function of the observed packet loss process with that of a normal wireless channel (i.e., $f_c(i)$), one can accurately identify the cause of the packet drops.

The benefit of exploiting the correlation of lost packets can be better illustrated by examining the insufficiency of the conventional method that relies only on the distribution of the number of lost packets. More specifically, under the conventional method, malicious-node detection is modeled as a binary hypothesis test, where H_0 is the hypothesis that there is no malicious node in a given link (all packet losses are due to link errors) and H_1 denotes there is a malicious node in the given link (packet losses are due to both link errors and malicious drops). Let z be the observed number of lost packets on the link during some interval t. Then,

$$z = \begin{cases} x, & \text{under } H_0 \text{ (no malicious nodes)} \\ x + y, & \text{under } H_1 \text{(there is a malicious node)}, \end{cases} \tag{1}$$

where x and y are the numbers of lost packets caused by link errors and by malicious drops, respectively. Both x and y are random variables. Let the probability density functions of z conditioned on H_0 and on H_1 be $h_0(z)$ and $h_1(z)$, respectively, as shown in Fig. 3a. We are interested in the maximum-uncertainty scenario where the a priori probabilities are given by $\Pr\{H_0\} = \Pr\{H_1\} = 0.5$, i.e., the auditor has no prior knowledge of the distributions of H_0 and H_1 to make any biased decision regarding the presence of malicious nodes. Let the false-alarm and miss-detection probabilities be P_{fa} and P_{md}, respectively. The optimal decision strategy that minimizes the total detection error $P_{de}\text{def}{=}0.5(P_{fa} + P_{md})$ is the maximum-likelihood (ML) algorithm:

$$\begin{cases} \text{if } z \leq z_{th}, & \text{accept } H_0, \\ \text{otherwise}, & \text{accept } H_1, \end{cases} \tag{2}$$

where the threshold z_{th} is the solution to the equation $h_0(z_{th}) = h_1(z_{th})$. Under this strategy, P_{fa} and P_{md} are the areas of the shaded regions shown in Fig. 3a, respectively. The problem with this mechanism is that, when the mean of y is small, $h_1(z)$ and $h_0(z)$ are not sufficiently separated, leading to large P_{fa} and P_{md}, as shown in Fig. 3b. This observation implies that when malicious packet drops are highly selective, counting the number of lost packets is not sufficient to accurately differentiate between malicious drops and link

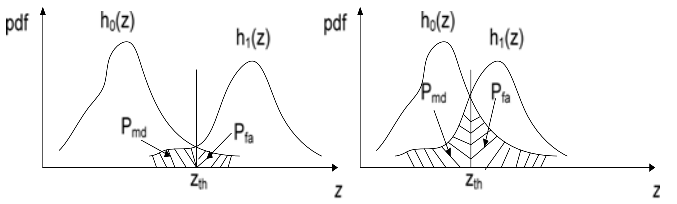

(a) mean of y much greater than mean of x (b) mean of y is comparable to mean of x

Fig. 3. Insufficiency of conventional detection algorithms when malicious packet drops are highly selective.

errors. For such a case, we use the correlation between lost packets to form a more informative decision statistic.

To correctly calculate the correlation between lost packets, it is critical to enforce a truthful packet-loss bitmap report by each node. We use HLA cryptographic primitive for this purpose. The basic idea of our method is as follows. An HLA scheme allows the source, which has knowledge of the HLA secret key, to generate HLA signatures $s_1, \ldots, s_M$ for M independent messages $r_1, \ldots, r_M$, respectively. The source sends out the r_i's and s_i's along the route. The HLA signatures are made in such a way that they can be used as the basis to construct a valid HLA signature for any arbitrary linear combination of the messages, $\sum_{i=1}^{M} c_i r_i$, without the use of the HLA secret key, where c_i's are randomly chosen coefficients. A valid HLA signature for $\sum_{i=1}^{M} c_i r_i$ can be constructed by a node that does not have knowledge of the secret HLA key if and only if the node has full knowledge of $s_1, \ldots, s_M$. So, if a node with no knowledge of the HLA secret key provides a valid signature for $\sum_{i=1}^{M} c_i r_i$, it implies that this node must have received all the signatures $s_1, \ldots, s_M$. Our construction ensures that s_i and r_i are sent together along the route, so that knowledge of $s_1, \ldots, s_M$ also proves that the node must have received $r_1, \ldots, r_M$.

Our detection architecture consists of four phases: setup, packet transmission, audit, and detection. We elaborate on these phases in the next section.

4.2 Scheme Details

4.2.1 Setup Phase

This phase takes place right after route P_{SD} is established, but before any data packets are transmitted over the route. In this phase, S decides on a symmetric-key crypto-system $(encrypt_{key}, decrypt_{key})$ and K symmetric keys $key_1, \ldots, key_K$, where $encrypt_{key}$ and $decrypt_{key}$ are the keyed encryption and decryption functions, respectively. S securely distributes $decrypt_{key}$ and a symmetric key key_j to node n_j on P_{SD}, for $j = 1, \ldots, K$. Key distribution may be based on the public-key crypto-system such as RSA: S encrypts key_j using the public key of node n_j and sends the cipher text to n_j. n_j decrypts the cipher text using its private key to obtain key_j. S also announces two hash functions, H_1 and H^{MAC}_{key}, to all nodes in P_{SD}. H_1 is unkeyed while H^{MAC}_{key} is a keyed hash function that will be used for message authentication purposes later on.

Besides symmetric key distribution, S also needs to set up its HLA keys. Let $e : G \times G \rightarrow G_T$ be a computable bilinear map with multiplicative cyclic group G and support $\mathbf{Z}_p$, where p is the prime order of G, i.e., for all α, $\beta \in G$ and q_1,

$q_2 \in \mathbf{Z}_p$, $e(\alpha^{q_1}, \beta^{q_2}) = e(\alpha, \beta)^{q_1 q_2}$. Let g be a generator of G. $H_2(.)$ is a secure map-to-point hash function: $\{0,1\}^* \rightarrow G$, which maps strings uniformly to G. S chooses a random number $x \in \mathbf{Z}_p$ and computes $v = g^x$. Let u be another generator of G. The secret HLA key is $sk = x$ and the public HLA key is a tuple $pk = (v, g, u)$.

4.2.2 Packet Transmission Phase

After completing the setup phase, S enters the packet transmission phase. S transmits packets to P_{SD} according to the following steps.

Before sending out a packet P_i, where i is a sequence number that uniquely identifies P_i, S computes $r_i = H_1(P_i)$ and generates the HLA signatures of r_i for node n_j, as follows:

$$s_{ji} = \left[H_2(i||j)u^{r_i}\right]^x, \quad \text{for } j = 1, \dots, K, \tag{3}$$

where $||$ denotes concatenation. These signatures are then sent together with P_i to the route by using a one-way chained encryption that prevents an upstream node from deciphering the signatures intended for downstream nodes. More specifically, after getting s_{ji} for $j = 1, \dots, K$, S iteratively computes the following:

$$\begin{aligned} \tilde{s}_{Ki} &= encrypt_{key_K}(s_{Ki}), \\ \tau_{Ki} &= \tilde{s}_{Ki}||MAC_{key_K}(\tilde{s}_{Ki}), \\ \tilde{s}_{K-1i} &= encrypt_{key_{K-1}}(s_{K-1i}||\tau_{Ki}), \\ \tau_{K-1i} &= \tilde{s}_{K-1i}||MAC_{key_{K-1}}(\tilde{s}_{K-1i}), \\ &\vdots \\ \tilde{s}_{ji} &= encrypt_{key_j}(s_{ji}||\tau_{j+1i}), \\ \tau_{ji} &= \tilde{s}_{ji}||MAC_{key_j}(\tilde{s}_{ji}), \\ &\vdots \\ \tilde{s}_{1i} &= encrypt_{key_1}(s_{1i}||\tau_{2i}), \\ \tau_{1i} &= \tilde{s}_{1i}||MAC_{key_1}(\tilde{s}_{1i}), \end{aligned} \tag{4}$$

where the message authentication code (*MAC*) in each stage j is computed according to the hash function $H^{MAC}_{key_j}$. After getting τ_{1i}, S puts $P_i||\tau_{1i}$ into one packet and sends it to node n_1.

When node n_1 receives the packet from S, it extracts P_i, $\tilde{s}_{1i}$, and $MAC_{key_1}(\tilde{s}_{1i})$ from the received packet. Then, n_1 verifies the integrity of $\tilde{s}_{1i}$ by testing the following equality:

$$MAC_{key_1}(\tilde{s}_{1i}) = H^{MAC}_{key_1}(\tilde{s}_{1i}). \tag{5}$$

If the test is true, then n_1 decrypts $\tilde{s}_{1i}$ as follows:

$$decrypt_{key_1}(\tilde{s}_{1i}) = s_{1i}||\tau_{2i}. \tag{6}$$

Then, n_1 extracts s_{1i} and τ_{2i} from the decrypted text. It stores $r_i = H_1(P_i)$ and s_{1i} in its proof-of-reception database for future use. This database is maintained at every node on P_{SD}. It can be considered as a FIFO queue of size M, which records the reception status for the most recent M packets sent by S. Finally, n_1 assembles $P_i||\tau_{2i}$ into one packet and relays this packet to node n_2. In case the test in (5) fails, n_1 marks the loss of P_i in its proof-of-reception database and does not relay the packet to n_2.

The above process is repeated at every intermediate node n_j, $j = 1, \dots, K$. As a result, node n_j obtains r_i and its HLA signature s_{ji} for every packet P_i that the node has received, and it relays $P_i||\tau_{j+1i}$ to the next hop on the route. The last hop, i.e., node n_K, only forwards P_i to the destination D. As proved in Theorem 4 in Section 4.3, the special structure of the one-way chained encryption construction in (4) dictates that an upstream node on the route cannot get a copy of the HLA signature intended for a downstream node, and thus the construction is resilient to the collusion model defined in Section 3.2. Note that here we consider the verification of the integrity of P_i as an orthogonal problem to that of verifying the tag τ_{ji}. If the verification of P_i fails, node n_1 should also stop forwarding the packet and should mark it accordingly in its proof-of-reception database.

4.2.3 Audit Phase

This phase is triggered when the public auditor A_d receives an ADR message from S. The ADR message includes the id of the nodes on P_{SD}, ordered in the downstream direction, i.e., $n_1, \dots, n_K$, S's HLA public key information $pk = (v, g, u)$, the sequence numbers of the most recent M packets sent by S, and the sequence numbers of the subset of these M packets that were received by D. Recall that we assume the information sent by S and D is truthful, because detecting attacks is in their interest. A_d conducts the auditing process as follows.

A_d submits a random challenge vector $\vec{c}_j = (c_{j1}, \dots, c_{jM})$ to node n_j, $j = 1, \dots, K$, where the elements c_{ji}'s are randomly chosen from $\mathbf{Z}_p$. Without loss of generality, let the sequence number of the packets recorded in the current proof-of-reception database be $P_1, \dots, P_M$, with P_M being the most recent packet sent by S. Based on the information in this database, node n_j generates a packet-reception bitmap $\vec{b}_j = (b_{j1}, \dots, b_{jM})$, where $b_{ji} = 1$ if P_i has been received by n_j, and $b_{ji} = 0$ otherwise. Node n_j then calculates the linear combination $r^{(j)} = \sum_{i=1, b_{ji} \neq 0}^{M} c_{ji} r_i$ and the HLA signature for the combination as follows:

$$s^{(j)} = \prod_{i=1, b_{ji} \neq 0} s_{ji}^{c_{ji}}. \tag{7}$$

Node n_j submits $\vec{b}_j$, $r^{(j)}$, and $s^{(j)}$ to A_d, as proof of the packets it has received.

A_d checks the validity of $r^{(j)}$ and $s^{(j)}$ by testing the following equality:

$$e(s^{(j)}, g) = e\left(\prod_{i=1, b_{ji} \neq 0}^{M} H_2(i||j)^{c_{ji}} u^{r^{(j)}}, v\right). \tag{8}$$

If the equality holds, then A_d accepts that node n_j received the packets as reflected in $\vec{b}_j$. Otherwise, A_d rejects $\vec{b}_j$ and judges that not all packets claimed in $\vec{b}_j$ are actually received by n_j, so n_j is a malicious node. We prove the correctness of this auditing algorithm in Section 4.3.

Note that the above mechanism only guarantees that a node cannot understate its packet loss, i.e., it cannot claim the reception of a packet that it actually did not receive. This mechanism cannot prevent a node from overly stating its packet loss by claiming that it did not receive a packet that it actually received. This latter case is prevented by another mechanism discussed in the detection phase.

4.2.4 Detection Phase

The public auditor A_d enters the detection phase after receiving and auditing the reply to its challenge from all nodes on P_{SD}. The main tasks of A_d in this phase include the following: detecting any overstatement of packet loss at each node, constructing a packet-loss bitmap for each hop, calculating the autocorrelation function for the packet loss on each hop, and deciding whether malicious behavior is present. More specifically, A_d performs these tasks as follows.

Given the packet-reception bitmap at each node, $\vec{b}_1, \ldots, \vec{b}_K$, A_d first checks the consistency of the bitmaps for any possible overstatement of packet losses. Clearly, if there is no overstatement of packet loss, then the set of packets received at node $j+1$ should be a subset of the packets received at node j, for $j = 1, \ldots, K-1$. Because a normal node always truthfully reports its packet reception, the packet-reception bitmap of a malicious node that overstates its packet loss must contradict with the bitmap of a normal downstream node. Note that there is always at least one normal downstream node, i.e., the destination D. So A_d only needs to sequentially scan $\vec{b}_j$'s and the report from D to identify nodes that are overstating their packet losses.

After checking for the consistency of $\vec{b}_j$'s, A_d starts constructing the per-hop packet-loss bitmap $\vec{m}_j$ from $\vec{b}_{j-1}$ and $\vec{b}_j$. This is done sequentially, starting from the first hop from S. In each step, only packets that are lost in the current hop will be accounted for in m_j. The packets that were not received by the upstream node will be marked as "not lost" for the underlying hop. Denoting the "lost" packet by 0 and "not lost" by 1, $\vec{m}_j$ can be easily constructed by conducting a bit-wise complement-XOR operation of $\vec{b}_{j-1}$ and $\vec{b}_j$. For example, consider the following simple case with three intermediate nodes (four hops) on the route and with $M = 10$. Suppose that $\vec{b}_1 = (0,1,1,1,1,1,1,1,0,1)$, $\vec{b}_2 = (0,1,1,1,1,1,1,1,0,1)$, $\vec{b}_3 = (0,1,0,1,1,0,1,1,0,1)$, and the destination D reports that $\vec{b}_D = (0,1,0,1,1,0,1,1,0,1)$. Then the per-hop packet-loss bitmaps are given by $\vec{m}_1 = (0,1,1,1,1,1,1,1,0,1)$, $\vec{m}_2 = (1,1,1,1,1,1,1,1,1,1)$, $\vec{m}_3 = (1,1,0,1,1,0,1,1,1,1)$, and $\vec{m}_4 = (1,1,1,1,1,1,1,1,1,1)$.

The auditor calculates the autocorrelation function γ_j for each sequence $\vec{m}_j = (m_{j1}, \ldots, m_{jM})$, $j = 1, \ldots, K$, as follows:

$$\gamma_j(i) = \frac{\sum_{k=1}^{M-i} m_{jk} m_{jk+i}}{M-i}, \quad \text{for } i = 0, \ldots, M-1; j = 1, \ldots, K. \tag{9}$$

The auditor then calculates the relative difference between γ_j and the ACF of the wireless channel f_c as follows:

$$\epsilon_j = \sum_{i=0}^{M-1} \frac{|\gamma_j(i) - f_c(i)|}{f_c(i)}. \tag{10}$$

The relative difference ϵ_j is then used as the decision statistic to decide whether or not the packet loss over the jth hop is caused by malicious drops. In particular, if $\epsilon_j \geq \epsilon_{th}$, where ϵ_{th} is an error threshold, then A_d decides that there is malicious packet drop over the hop. In this case, both ends of the hop will be considered as suspects, i.e., either the transmitter did not send out the packet or the receiver chose to ignore the received packet. S may choose to exclude both nodes from future packet transmissions, or alternatively, apply a more extensive investigation to refine its detection. For example, this can be done by combining the neighbor-overhearing techniques [12] used in the reputation system. By fusing the testimony from the neighbors of these two nodes, A_d can pin-point the specific node that dropped the packet. Once being detected, the malicious node will be marked and excluded from the route to mitigate its damage.

The above detection process applies to one end-to-end path. The detection for multiple paths can be performed as multiple independent detections, one for each path. Although the optimal error threshold that minimizes the detection error is still an open problem, our simulations show that through trial-and-error, one can easily find a good ϵ_{th} that provides a better detection accuracy than the optimal detection scheme that utilizes only the pdf of the number of lost packets.

Public verifiability. After each detection, A_d is required to publish the information it received from involved nodes, i.e., $\vec{b}_j$, $r^{(j)}$, $s^{(j)}$, for $j \in P_{SD}$, so that a node can verify all calculation has been performed correctly. Note that no knowledge of the HLA secret key x is required in the verification process. At the same time, because A_d has no knowledge of x, there is no way for it to forge a valid HLA signature for $r^{(j)}$. In other words, A_d cannot claim a misbehaving node to be a normal one. Furthermore, the privacy-preserving property of the scheme (see Theorem 4 in Section 4.3) ensures that publishing the auditing information will not compromise the confidentiality of the communication.

4.3 Security Analysis

We prove that the proposed scheme has the following security properties.

Theorem 1. *The verification of $r^{(j)}$ and $s^{(j)}$, as specified in (8), is correct, i.e., (8) must hold for a $(\vec{c}_j, r^{(j)}, s^{(j)})$ tuple that is constructed according to the specification presented in Section 4.2.3.*

Proof. The correctness of (8) is shown as follows:

$$\begin{aligned} e(s^{(j)}, g) &= e\left(\prod_{i=1, b_{ji}\neq 0}^{M} s_{ji}^{c_{ji}}, g\right) \\ &= e\left(\prod_{i=1, b_{ji}\neq 0}^{M} \left\{H_2(i||j)u^{r_i}\right\}^{x c_{ji}}, g\right) \\ &= e\left(\prod_{i=1, b_{ji}\neq 0}^{M} \left\{H_2(i||j)u^{r_i}\right\}^{c_{ji}}, g\right)^x \\ &= e\left(\prod_{i=1, b_{ji}\neq 0}^{M} H_2(i||j)^{c_{ji}} u^{c_{ji} r_i}, g\right)^x \\ &= e\left(\prod_{i=1, b_{ji}\neq 0}^{M} H_2(i||j)^{c_{ji}} u^{r^{(j)}}, g^x\right) \\ &= e\left(\prod_{i=1, b_{ji}\neq 0}^{M} H_2(i||j)^{c_{ji}} u^{r^{(j)}}, v\right). \end{aligned} \tag{11}$$

So Theorem 1 holds. □

Theorem 2. *The construction specified in Section 4.2 is secure under the collusion model defined in Section 3.2, i.e., an adversary that does not receive a packet P_i cannot claim receiving this packet in its $\vec{b}_j$ by forging a HLA signature for a random linear combination of the received packets, even if this adversary colludes with any other malicious node in P_{SD}.*

Proof. For a given node n_j, our construction essentially follows the BLS-signature-based HLA construction described in [27]. Under the implicitly assumed condition of no collusion between attackers, the authors in [27] proved that the construction is secure, i.e., no adversary can forge a response to a random challenge if it does not know the HLA signature of each packet in the linear combination. So here, we only need to show that collusion between malicious nodes does not give the attacker more information about the HLA signature of the packets. This can be shown by observing the following novel properties of our HLA construction:

1) For a packet P_i, the signature scheme specified in (3) dictates that its HLA signature s_{ji} is not only tied to the packet sequence number (i), but also related to the node index (j) that is relaying the packet. This means that for the same packet, each hop on P_{SD} is given a different HLA signature. The verification scheme in (8) accounts for both i and j. In the no-collusion case, by treating the concatenation of $(i||j)$ as a meta packet sequence number, the security of our construction can be proved in the same way as that in [27].
2) The way that the HLA signatures are distributed to nodes on P_{SD}, as specified in (4), dictates that an upstream node n_j cannot get a copy of the HLA signature $s_{j'i}$ of a downstream node $n_{j'}$, where $j < j' \leq K$, unless the downstream node $n_{j'}$ receives the signature $s_{j'i}$ *first on* P_{SD} and then sends it through the covert channel to the upstream node n_j. Therefore, there is no way for a downstream malicious node to get any information on its HLA signature if the upstream attacker drops the packet. As a result, the secret information exchange on the covert channel does not help the adversary to get more information on its HLA signature than the scenario where there is no collusion.

Combining the above arguments, Theorem 2 is proved. □

Theorem 3. *The proposed scheme ensures that the packet-reception bitmap reported by a node in P_{SD} is truthful.*

The validity of Theorem 3 is straightforward, because Theorem 2 guarantees that the node cannot understate its packet loss information. At the same time, from our discussion in Section 4.2.4, it is clear that a malicious node cannot overstate its packet loss either. So a node must report its actual packet reception information truthfully to A_d.

Theorem 4. *Our HLA construction is publicly verifiable and privacy preserving, i.e., the auditor A_d does not require the secret key of the HLA scheme to verify a node's response. In addition, A_d cannot determine the content of the packets transmitted over P_{SD} from the information submitted by nodes.*

Proof. Public verifiability is clear from the construction of the scheme. The privacy-preserving property is guaranteed by the application of the secure hash function H_1. More specifically, instead of directly computing the HLA signature for a packet P_i, our construction computes the signature for the image of the packet $r_i = H_1(P_i)$. During the auditing phase, A_d can collect a set of linear combinations of r_i's. So it is possible for A_d to calculate r_i's by solving a set of linear equations, if a sufficient number of combinations are collected. Even if A_d can recover r_i, it should not be able to guess P_i because of H_1's resilience to the pre-image attack. □

4.4 Overhead Analysis

The proposed scheme requires relatively high computation capability at the source, but incurs low communication and storage overheads along the route, as explained below.

4.4.1 Computation Requirements

Most of the computation is done at the source node (for generating HLA signatures) and at the public auditor (for conducting the detection process). We consider the public auditor as a dedicated service provider that is not constrained by its computing capacity. So the computational overhead should not be a factor limiting the application of the algorithm at the public auditor. On the other hand, the proposed algorithm requires the source node to generate K HLA signatures for a K-hop path for each data packet. The generation of HLA signatures is computationally expensive, and may limit the applicability of the algorithm. We propose a block-based HLA signature and detection mechanism in Section 5, whereby the processing is based on block of packets rather than individual packets, to reduce this computation overhead by multiple folds. We evaluate the performance of the proposed mechanism by extensive simulations in Section 6.2.4.

4.4.2 Communication Overhead

The communication overhead for the setup phase is a one-time cost, incurred when P_{SD} is established. Here we mainly focus on the recurring cost during the packet transmission and auditing phases (there is no communication overhead in the detection phase). For a transmitted packet P_i, S needs to send one encrypted HLA signature and one MAC to each intermediate node on P_{SD}. Our HLA signature follows the BLS scheme in [7]. So an HLA signature s_{ij} is 160-bit long. If encrypted by DES, the encrypted signature $\tilde{s}_{ij}$ is 192 bits in length (a block in DES is 64-bit long, so the length of the cipher text of DES is multiples of 64 bits). The MAC-related hash function H_{key}^{MAC} can be implemented in SHA-1 and has a length of 160 bits. So for each packet, the per-hop communication overhead incurred by the proposed scheme in the packet transmission phase is $192 + 160 = 352$ bits, or 44 bytes. For a path of K intermediate hops, the total communication overhead for transmitting a packet is $44K$ bytes. For example, when $K = 10$, the overhead is 440 bytes/packet. For an IEEE 802.11 system, this is about 19 percent of the maximum MSDU (2,304 bytes).

In the auditing phase, the auditor A_d sends a random challenge vector $\vec{c}_j$ to each node n_j. Let each element in this vector be a 32-bit integer. The challenge has a length of $4M$ bytes. Based on our simulation in Section 6, $M = 50$ is typically enough to achieve good detection accuracy. So this means each challenge can be delivered in one packet. Node n_j replies to the challenge with $\vec{b}_j$, $r^{(j)}$, and $s^{(j)}$. Among them, $\vec{b}_j$ is an M-bit bitmap. $r^{(j)}$ is the linear combination of the SHA-1 image of the packets, so $r^{(j)}$ also has a length of 160 bits. $s^{(j)}$ is an HLA signature of $r^{(j)}$, so it is also 160-bit long. Overall, the reply from a node to A_d has a length of $320 + M$ bits, which can also be delivered in one packet.

4.4.3 Storage Overhead

During its operation, a node n_j on P_{SD} needs to store the key key_j, the H_1 hash image, and the associated HLA signature for each of the M most recently received packets. Assuming $encrypt_{key}$ and $decrypt_{key}$ are based on DES, key_j has a length of 56 bits. Let the hash function H_1 be based on SHA-1. So the H_1 image of a packet is 160-bit long. The HLA signature is based on BLS (Boneh-Lynn-Shacham) scheme [7] and is 160-bit long. So in total the storage overhead at n_j is $320M + 56$ bits, or $40M + 7$ bytes. This storage overhead is quite low. For example, when $M \leq 50$, the storage overhead at a node is less than 2 KB.

5 Reducing Computation Overhead: Block-Based HLA Signature Generation and Detection

As discussed in Section 4.4.1, one major limitation of the proposed baseline HLA detection algorithm is the high computation overhead of the source node. In this section, we proposed a block-based solution that can reduce this overhead by multiple folds. The main idea is to make the HLA signature scalable: instead of generating per-packet HLA signatures, per-block HLA signatures will be generated, where a block consists of $L > 1$ packets. Accordingly, the detection will be extended to blocks, and each bit in the packet-loss bitmap represents a block of packets rather than a single packet. The details of this extension are elaborated as follows.

In the Packet Transmission Phase, rather than generating HLA signatures for every packet, now the signatures are based on a block of packets. In particular, L consecutive packets are deemed as one block. Accordingly, the stream of packets is now considered as stream of blocks. Denote the L packets in block i as $P_{i1}, \ldots, P_{iL}$, respectively. The source S generates block-HLA signatures for block i as follows:

1) S computes $r_i = H_1(P_{i1})$. S then computes HLA signatures of r_i for node n_j, say s_{ji}, where $j = 1, \ldots, K$, according to (3).
2) For each node n_j, S generates L random numbers $\kappa_{ji}^{(1)}, \ldots, \kappa_{ji}^{(L)} \in \mathbf{Z}_p$, such that $\sum_{l=1}^{L} \kappa_{ji}^{(l)} = s_{ji}$. This could be done, e.g., but first generating $L-1$ arbitrary numbers and then make the Lth number equal to $s_{ji} - \sum_{l=1}^{L-1} \kappa_{ji}^{(l)}$.
3) For packet P_{il}, S assigns $\kappa_{ji}^{(l)}$'s, $j = 1, \ldots, K$, as the block-HLA signatures for node $1, \ldots, K$, respectively. These signatures are then transmitted with packet P_{il} by following the one-way chained encryption and decryption scheme described in (4) through (6).

In line with the above block-HLA signatures, a node n_j is able to compute $s_{ji} = \sum_{l=1}^{L} \kappa_{ji}^{(l)}$ if and only if it receives all L packets of block i. Node n_j stores r_i and s_{ji} in its proof-of-reception database as the proof for block i.

Auditing is now based on blocks. In particular, at node n_j, suppose the sequence number of the blocks recorded in the proof-of-reception database are $B_1, \ldots, B_M$. Based on the information in the database, node n_j generates a block-reception bitmap $\vec{b}_j = (b_{j1}, \ldots, b_{jM})$, where $b_{ji} = 1$ if and only if all L packets in block B_i has been received by n_j, and $b_{ji} = 0$ otherwise. Except the above, A_d still follows the same algorithm in Section 4.2.3 to submit random challenge, receive response, and verify the truthfulness of the reported block-reception bitmap.

In the detection phase, the ACF of the wireless channel needs to be coarsened such that one unit of lag represents L consecutive packets. This could be done by first coarsening the packet reception bitmap observed in the training phase using blocks: L consecutive 1's are mapped to a 1 in the blocked-based bitmap, otherwise a 0 will be mapped. The ACF of the coarsened wireless channel is then compared with the ACF of the block-reception bitmap reported by each node to detect possible malicious packet drops.

From the above description, it is clear that the block-based HLA signature and detection mechanism can in general reduce the computation overhead by L folds. However, the coarser representation of lost packets makes it difficult to accurately capture the correlation between them. For example, even with a small block size, say $L = 2$, it is not possible to tell whether a block loss is due to the loss of one packet or both packets in the block, which correspond to very different packet-loss correlations. Therefore, it is expected that the reduced computational overhead comes at the cost of less detection accuracy. We study the performance of the block-based algorithm in Section 6.2.4.

6 Performance Evaluation

6.1 Simulation Setup

In this section, we compare the detection accuracy achieved by the proposed algorithm with the optimal maximum likelihood algorithm, which only utilizes the distribution of the number of lost packets. For given packet-loss bitmaps, the detection on different hops is conducted separately. So, we only need to simulate the detection of one hop to evaluate the performance of a given algorithm. We assume packets are transmitted continuously over this hop, i.e., a saturated traffic environment. We assume channel fluctuations for this hop follow the Gilbert-Elliot model, with the transition probabilities from good to bad and from bad to good given by P_{GB} and P_{BG}, respectively. We consider two types of malicious packet dropping: random dropping and selective dropping. In the random dropping attack, a packet is dropped at the malicious node with

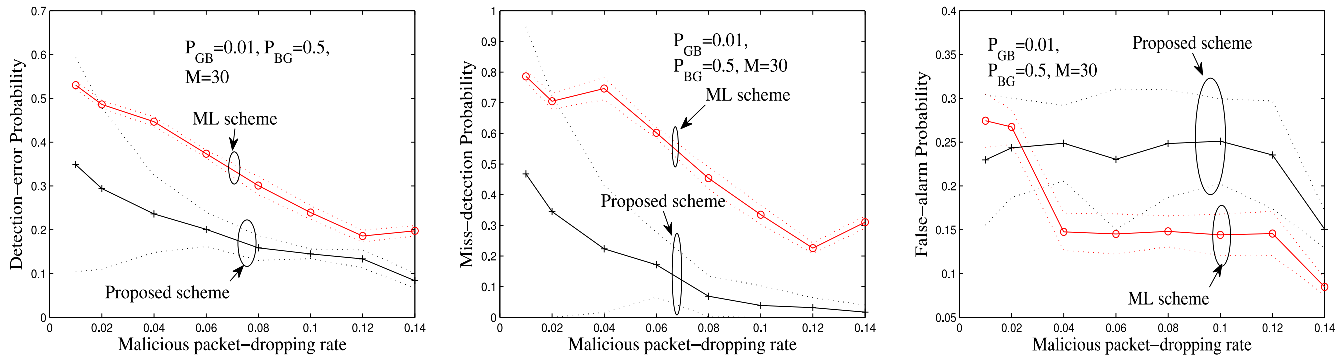

(a) Overall detection-error probability (b) Miss-detection probability (c) False-alarm probability

Fig. 4. Detection accuracy versus P_M (random packet-drop case).

probability P_M. In the selective dropping attack, the adversary drops packets of certain sequence numbers. In our simulations, this is done by dropping the middle N of the M most recently received packets, i.e., setting the N bits in the middle of the packet-loss bitmap to 0 (if a packet in these positions is dropped due to link errors, then the set of 0's extends to an extra bit in the middle). P_M and N are simulation parameters that describe the selectivity of the attack. In both cases, we let $\epsilon_{th} = 10\%$ for the proposed algorithm.

We are interested in the following three performance metrics: probability of false alarm (P_{fa}), probability of miss-detection (P_{md}), and the overall detection-error probability (P_{error}). We collect these statistics as follows. In each run, we first simulate 1,000 independently generated packet-loss bitmaps for the hop, where packet losses are caused by link errors only. We execute our detection algorithm over these packet-loss bitmaps and collect the number of cases where the algorithm decides that an attacker is present. Let this number be I_{fa}. P_{fa} of this run is calculated as $P_{fa} = I_{fa}/1{,}000$. We then simulate another 1,000 independently generated packet-loss bitmaps, where losses are now caused by both link errors and malicious drops. Let the number of cases where the detection algorithm rules that an attacker is not present be I_{md}. P_{md} of the underlying run is given by $P_{md} = I_{md}/1{,}000$. P_{error} is given by $P_{error} = (I_{fa} + I_{md})/2{,}000$. The above simulation is repeated 30 times, and the mean and 95 percent confidence interval are computed for the various performance metrics.

6.2 Results

6.2.1 Random Packet Dropping

The detection accuracy is shown in Fig. 4 as a function of the malicious random-drop rate P_M. In each subfigure, there are two sets of curves, representing the proposed algorithm and the optimal ML scheme, respectively. In each set of curves, the one in the middle represents the mean, and the other two represent the 95 percent confidence interval. In general, the detection accuracy of both algorithms improves with P_M (i.e., the detection error decreases with P_M). This is not surprising, because malicious packet drops become more statistically distinguishable as the attacker starts to drop more packets. In addition, this figure shows that for $\epsilon_{th} = 10\%$, the proposed algorithm provides slightly higher false-alarm rate (subfigure (c)) but significantly lower miss-detection probability (subfigure (b)) than the ML scheme. A low miss-detection probability is very desirable in our context, because it means a malicious node can be detected with a higher probability. The slightly higher false-alarm rate should not be a problem, because a false alarm can be easily recognized and fixed in the post-detection investigation phase. Most importantly, the overall detection-error probability of the proposed scheme is lower than that of the ML scheme (subfigure (a)). We are especially interested in the regime when P_M is comparable to the average packet loss rate due to link errors, given by $\frac{P_{GB}}{P_{GB}+P_{BG}} = \frac{0.01}{0.01+0.5} \approx 0.02$. This regime represents the scenario in which the attacker hides its drops in the background of link errors by mimicking the channel-related loss rate. In this case, the ML scheme cannot correctly differentiate between link errors and malicious drops. For example, when $P_M = 0.01$, the ML scheme results in $P_{md} = 80\%$ and $P_{fa} = 23\%$. This is close to arbitrarily ruling that every packet loss is due to link error only, leading to an overall detection-error rate of 50 percent (see subfigure (a)). Our proposed algorithm, on the other hand, achieves a much better detection accuracy, because its P_{md} and P_{fa} are both lower than those under the ML scheme. As a result, when $P_M = 0.01$, the total detection-error rate of the proposed algorithm is about 35 percent. When P_M is increased to 0.04, P_{error} of the proposed scheme reduces to only 20 percent, which is roughly half of the error rate of the ML scheme at the same P_M. Remembering that the detection-error rate of the ML scheme is the lowest among all detection schemes that only utilize the distribution of the number of lost packets, the lower detection-error rate of the proposed scheme shows that exploiting the correlation between lost packets helps in identifying the real cause of packet drops more accurately. The effect of exploiting the correlation is especially visible when the malicious packet-drop rate is comparable with the link error rate. Meanwhile, we also note that the 95 percent confidence interval of the proposed scheme is wider than that of the ML scheme. This is because the decision variable ϵ_j in the proposed scheme is a second-order function of the random packet loss process, while the decision variable in the ML scheme (i.e., number of lost packets) is a first order function of the same packet loss process. As a result, the decision variable of the proposed scheme possesses more randomness than that of the ML scheme, as reflected by the wider 95 percent confidence interval.

In Fig. 5, we plot the detection accuracy as a function of the size of the packet-loss bitmap (M). It can be

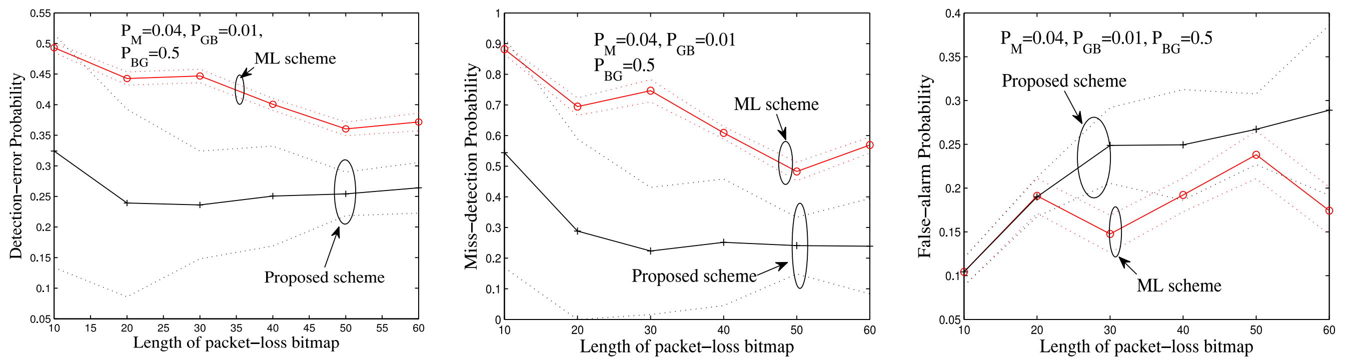

(a) Overall detection-error probability (b) Miss-detection probability (c) False-alarm probability

Fig. 5. Detection accuracy versus M (random packet-drop case).

observed that P_{error} for the proposed scheme decreases with M. However, as M becomes sufficiently large, e.g., $M = 30$ in our case, a further increase in the size of the bitmap does not lead to additional improvement in the detection accuracy. This can be explained by noting that the two-state Markovian GE channel model has a short-range dependence, i.e., the correlation between two points of the fluctuation process decays rapidly with the increase in the separation between these points. This short-range dependence is reflected in an exponentially decaying autocorrelation function for the channel. As a result, a good estimation of the autocorrelation function can be derived as long as M is long enough to cover the function's short tail. This phenomenon implies that a node does not need to maintain a large packet-reception database in order to achieve a good detection accuracy under the proposed scheme. It also explains the low storage overhead incurred by our scheme.

The detection accuracy is plotted in Fig. 6 as a function of the channel state transition rate P_{GB}. It can be observed from this figure that P_{error} for both algorithms increases with P_{GB}. This is not surprising because at its initial point of $P_{GB} = 0.01$, the expected link error rate is about 0.02, which is much smaller than the malicious packet drop rate of $P_M = 0.1$. So it is relatively easy to differentiate between the case where packet drops are caused by link errors only and the one where such drops are caused by the combined effect of link errors and malicious drops. As P_{GB} increases, the link error probability approaches P_M, making the statistical separation of the two cases harder. As a result, the detection error increases with P_{GB}. For all values of P_{GB} in this figure, the proposed algorithm always achieves significantly lower detection-error probability than the ML scheme.

6.2.2 Selective Packet Dropping

The detection error as a function of the number of maliciously dropped packets is shown in Fig. 7. At the low end of the x-axis, maliciously dropped packets account for only $1/50 = 2\%$ of the total packets in the packet-loss bitmap. This is identical to the link error rate of 0.02, assumed in the simulation. Similar performance trends can be observed to the case of the random packet dropping. Fewer detection errors are made by both algorithms when more packets are maliciously dropped. In all the simulated cases, the proposed algorithm can detect the actual cause of the packet drop more accurately than the ML scheme, especially when the number of maliciously dropped packets is small. When the number of maliciously dropped packets is significantly higher than that caused by link errors (greater than four packets in our simulation), the two algorithms achieve comparable detection accuracy. In this scenario, it may be wise to use the conventional ML scheme due to its simplicity (e.g., no need to enforce truthful reports from intermediate nodes, etc.).

The detection errors are plotted in Fig. 8 as a function of the size of the packet-loss bitmap (M). To conduct a fair comparison, as we increase M, we also increase the number of maliciously dropped packets, so as to maintain a malicious packet-dropping rate of 10 percent. It can be observed that a small M is enough to achieve good detection accuracy

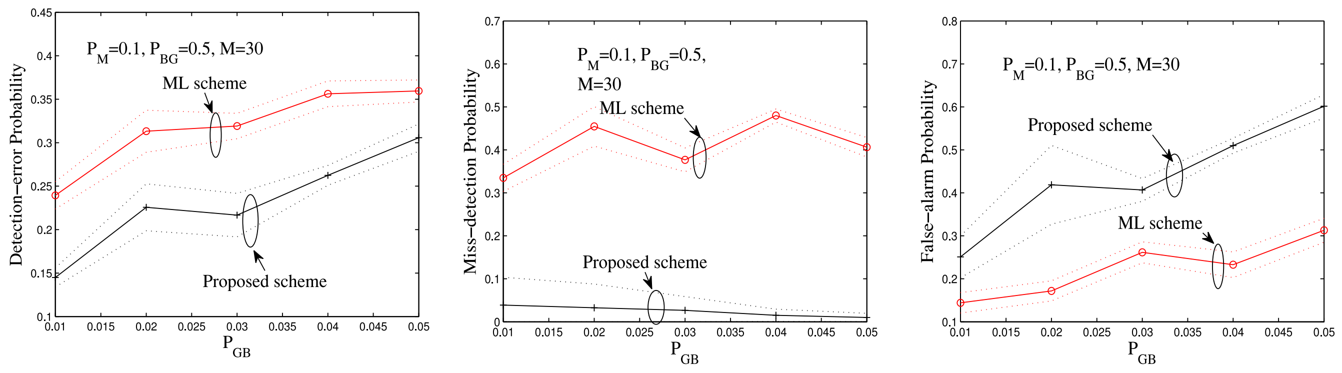

(a) Overall detection-error probability (b) Miss-detection probability (c) False-alarm probability

Fig. 6. Detection accuracy versus P_{GB} (random packet-drop case).

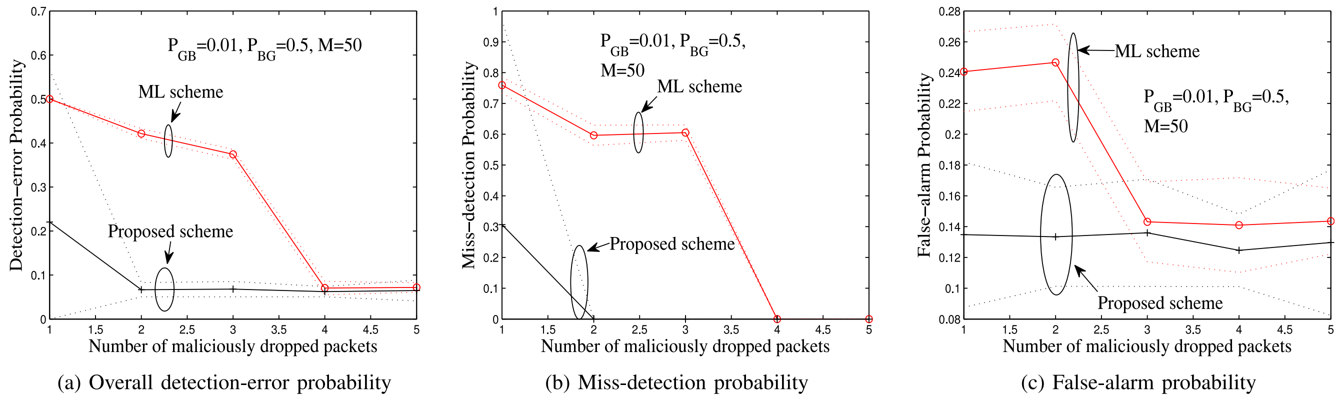

Fig. 7. Detection accuracy versus number of maliciously dropped packets (selective packet-drop case).

under the proposed scheme, due to the short-range dependence property of the channel.

In Fig. 9, the detection errors are plotted as a function of the channel state transition probability P_{GB}. Similar trends are observed to those in the random packet dropping case, i.e., the algorithms make more detection errors when the link error rate approaches the malicious packet-drop rate. Once again, the proposed algorithm consistently outperforms the ML scheme in all the tested cases.

6.2.3 Dropping of Control Packets

Our simulations so far have not made any application-semantic (use case) assumption on the dropped packets. In reality, however, because these packets are usually used for control purposes, the loss of these packets may generate significant impacts on the transmission of other (i.e., data) packets. In this series of simulations, we evaluate how the correlation between the control and data packets affects the performance of the proposed scheme. In particular, we consider a multi-hop cognitive radio network, where control packets are exchanged over an end-to-end path to maintain channel synchronization between consecutive hops. A control packet contains the channel id that the two ends of a hop should tune to. The exchange of these packets could be end-to-end (i.e., the entire path operates over a channel commonly available to all hops) or local (the path consists of several segments, each of which operates over a different channel available only to the hops of that segment). In either case, the drop of a control packet will disrupt the frequency synchronization of a hop, so that data packets transmitted over the hop will be lost until the frequency synchronization is resumed by the next valid exchange of control packets. In this simulation, we assume that a random number of l_{data} data packets are sent between two consecutive control packets. We assume that l_{data} follows geometric distribution with mean parameter L_{data} (i.e., the continuous idle time of a channel is exponentially distributed, as commonly assumed in the cognitive radio literature). In addition, we also assume that an attacker uniformly randomly drops a certain percentage of the control packets. This percentage and L_{data} are parameters varied in the simulation. Finally, we use the same Gilbert-Elliot model as previous simulations to generate the wireless channel.

Fig. 10a plots detection accuracy as a function of the control packet dropping rate. It can be observed that under the correlated control and data packet losses, the proposed scheme achieves significantly better detection accuracy than the ML scheme for all tested control packet dropping rates, a similar trend to those observed when such correlation is not considered (e.g., see the random packet drops in Fig. 4a). Meanwhile, it can also be observed from Figs. 10a and 4a that, compared with the results of uncorrelated packet drops, the detection-error probability under correlated packet losses is in general smaller, indicating that the correlation between control and data packet losses may help to improve the detection accuracy. This is true for both schemes. This is because such correlation further amplifies the distinction between the statistics of the wireless channel and the malicious packet drops, making the detection easier.

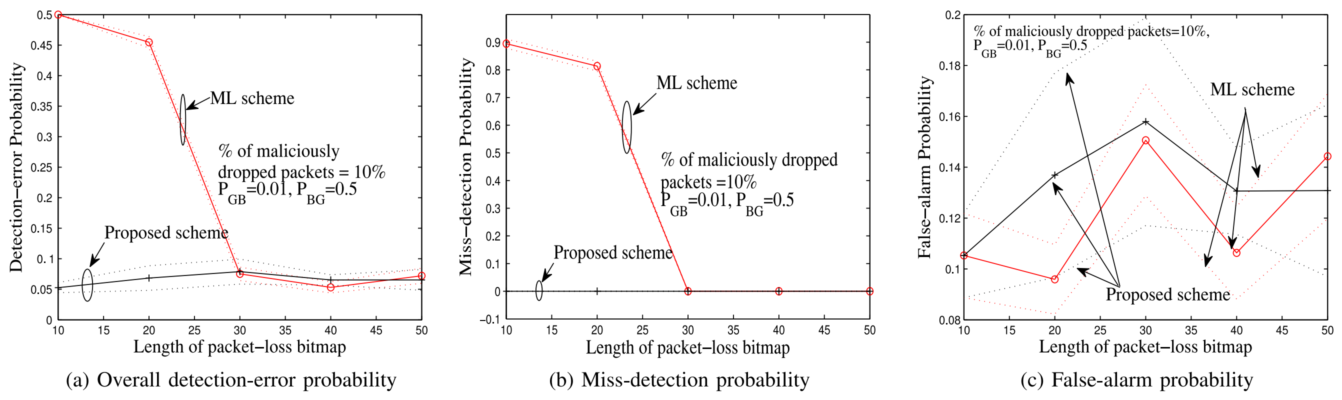

Fig. 8. Detection accuracy versus M (selective packet-drop case).

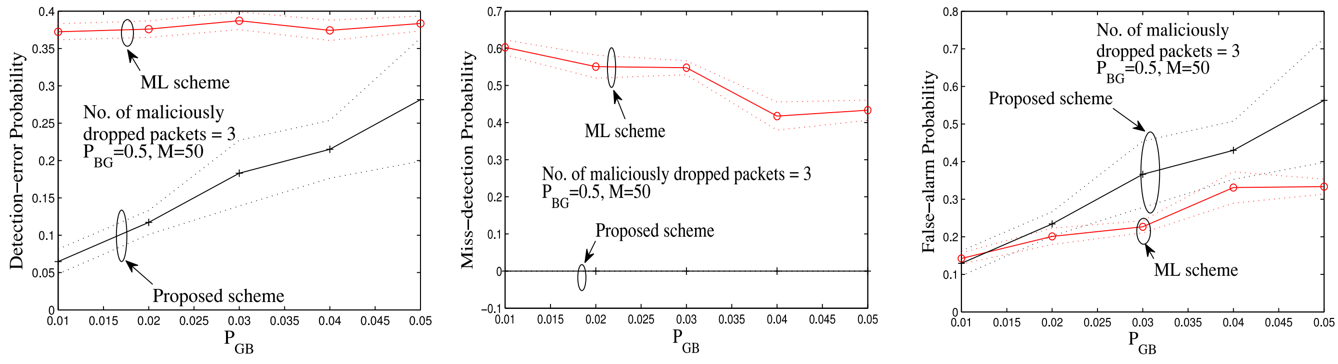

(a) Overall detection-error probability (b) Miss-detection probability (c) False-alarm probability

Fig. 9. Detection accuracy versus P_{GB} (selective packet-drop case).

We study the detection accuracy as a function of average number of data packets transmitted between two consecutive control packets (L_{data}) in Fig. 10b. It can be observed that this parameter has little impact on the ML scheme, because under a given control packet loss rate, the overall (control+data) packet loss rate does not change with L_{data}. ML scheme relies on detecting the number of lost packets, and thus is not affected by L_{data}. In contrast, the proposed scheme may benefit from a larger L_{data}: even if the average detection accuracy does not improve much, its 95 percent confidence interval shrinks significantly with L_{data}. This is explained by comparing the packet loss patterns of the wireless channel and the correlated packet drops. Specifically, on average two packets are lost in a row in a wireless link error (this is given by $1/(1-P_{BG}) = 1/0.5 = 2$), while on average L_{data} packets are lost under each malicious drop. Therefore, the distinction between the above two packet-loss patterns increases with L_{data}. The proposed scheme exploits such a distinction in patterns and thus can benefit from larger L_{data}.

In Fig. 10c we plot the detection-error probability as a function of channel state transition parameter P_{GB}. It can be observed that the detection accuracy deteriorates with the increase of P_{GB}, because it becomes more and more difficult to decide the actual source of packet loss when link error rate approaches the malicious packet dropping rate. Once again, the proposed scheme consistently achieves higher detection accuracy than ML scheme in all simulated cases.

6.2.4 Block-Based Detection

In this series of simulations, we study the detection accuracy of block-based algorithms as a function of block size. Fig. 11a plots the detection accuracy for random packet drops under two packet drop probabilities: high ($P_M = 0.08$) and low ($P_M = 0.01$). The performance of the ML scheme is also plotted in the same figure for comparison. In general, it shows that for both cases the detection error increases with the block size. This is expected, as a larger block size hides more details of packet losses, and therefore makes the actual correlation of lost packets more difficult to calculate. Meanwhile, the benefits of blocked-based algorithm is also observed: it is able to trade computation complexity for better detection accuracy. For example, under low packet dropping rate, it shows that the block-based algorithm can reduce the computation overhead of the baseline HLA detection by 10 folds, and still be able to achieve better detection accuracy than the ML scheme. At high packet dropping rate, the block-based algorithm can achieves a $4\times$ computation overhead reduction, while still achieving slightly better detection accuracy than the ML scheme.

Fig. 11b plots the detection accuracy for random packet drops under two packet sampling methods. In the first method, we fix the total number of packets used in the sample, and therefore the number of sampled blocks varies with the block size. In the second method, we fix the number of sampled blocks, but the number of sampled packets changes with the block size. Note that the amount of computation required to compute the block-based signatures decreases with the block size in the first method, but

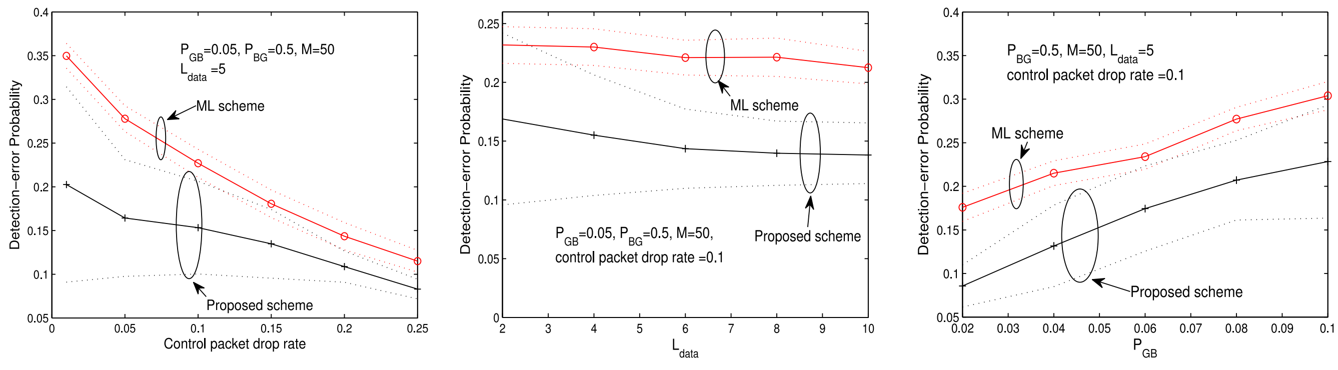

(a) Impact of control packet dropping rate (b) Impact of L_{data} (c) Impact of P_{GB}

Fig. 10. Detection accuracy for control packet drops.

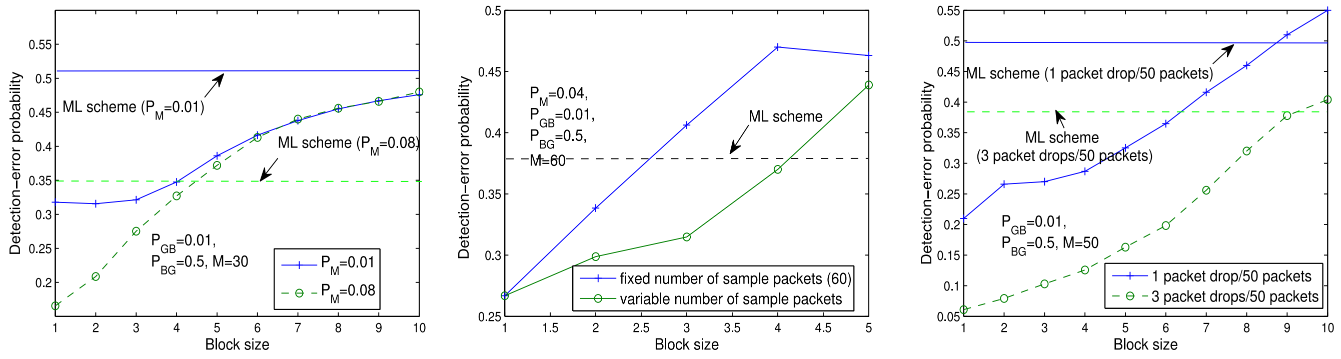

(a) Random packet drops

(b) Impact of sample packets (random packet drops)

(c) Selective packet drops

Fig. 11. Detection accuracy of block-based algorithms.

remains the same in the second method. The second method does not reduce the amount of computation, rather, it reduces the intensity of the computation by distributing it over a larger time interval (more packets). From this figure, it can be observed that under both methods, the detection accuracy deteriorates with the block size, but the deterioration is more severe under the first method. This is not surprising, because in method one the block-reception bitmap becomes shorter with the increase of block size, and therefore the computed ACF is less accurate, due to the insufficient sample size. Meanwhile, it can be observed that, at a detection accuracy comparable to that of the ML scheme, the second method achieves $4\times$ computation overhead reduction over the baseline algorithm, whereas the saving of the first method is only $2\times$. This observation suggests that, to maintain a good detection accuracy, block-based algorithm may be better used as a way to reduce the computation intensity of the source node, rather than a way to reduce the absolute amount of the computation.

Fig. 11c plots the detection accuracy for selective packet drops under two packet dropping rates: high (three out of every 50 packets are dropped) and low (one out of every 50 packets is dropped). A similar trend to Fig. 11a can be observed. This observation suggests that the property–block-based algorithm can trade computation complexity for detection accuracy—is universal (i.e., holds under various attack models).

7 Conclusions

In this paper, we showed that compared with conventional detection algorithms that utilize only the distribution of the number of lost packets, exploiting the correlation between lost packets significantly improves the accuracy in detecting malicious packet drops. Such improvement is especially visible when the number of maliciously dropped packets is comparable with those caused by link errors. To correctly calculate the correlation between lost packets, it is critical to acquire truthful packet-loss information at individual nodes. We developed an HLA-based public auditing architecture that ensures truthful packet-loss reporting by individual nodes. This architecture is collusion proof, requires relatively high computational capacity at the source node, but incurs low communication and storage overheads over the route. To reduce the computation overhead of the baseline construction, a packet-block-based mechanism was also proposed, which allows one to trade detection accuracy for lower computation complexity.

Some open issues remain to be explored in our future work. First, the proposed mechanisms are limited to static or quasi-static wireless ad hoc networks. Frequent changes on topology and link characteristics have not been considered. Extension to highly mobile environment will be studied in our future work. In addition, in this paper we have assumed that source and destination are truthful in following the established protocol because delivering packets end-to-end is in their interest. Misbehaving source and destination will be pursued in our future research. Moreover, in this paper, as a proof of concept, we mainly focused on showing the feasibility of the proposed cypto-primitives and how second-order statistics of packet loss can be utilized to improve detection accuracy. As a first step in this direction, our analysis mainly emphasize the fundamental features of the problem, such as the untruthfulness nature of the attackers, the public verifiability of proofs, the privacy-preserving requirement for the auditing process, and the randomness of wireless channels and packet losses, but ignore the particular behavior of various protocols that may be used at different layers of the protocol stack. The implementation and optimization of the proposed mechanism under various particular protocols will be considered in our future studies.

Acknowledgments

The work of T. Shu was supported in part by US National Science Foundation (NSF) under Grant CNS-1343156. The work of M. Krunz was supported by NSF (Grants CNS-1016943 and IIP-1265960) and by ARO (Grant W911NF-13-1-0302). Any opinions, findings, conclusions, or recommendations expressed in this paper are those of the author(s) and do not necessarily reflect the views of NSF or ARO. A preliminary version of this paper was presented in ACM WiSec 2012 Conference, Tucson, AZ, April 2012.

References

[1] J. N. Arauz, "*802.11 Markov channel modeling*," Ph.D. dissertation, School Inform. Sci., Univ. Pittsburgh, Pittsburgh, PA, USA, 2004.

[2] C. Ateniese, R. Burns, R. Curtmola, J. Herring, L. Kissner, Z. Peterson, and D. Song, "Provable data possession at untrusted stores," in *Proc. ACM Conf. Comput. and Commun. Secur.*, Oct. 2007, pp. 598–610.

[3] G. Ateniese, S. Kamara, and J. Katz, "Proofs of storage from homomorphic identification protocols," in *Proc. Int. Conf. Theory Appl. Cryptol. Inf. Security*, 2009, pp. 319–333.

[4] B. Awerbuch, R. Curtmola, D. Holmer, C. Nita-Rotaru, and H. Rubens, "ODSBR: An on-demand secure byzantine resilient routing protocol for wireless ad hoc networks," *ACM Trans. Inform. Syst. Security*, vol. 10, no. 4, pp. 1–35, 2008.

[5] B. Awerbuch, R. Curtmola, D. Holmer, C. Nita-Rotaru, and H. Rubens, "ODSBR: An on-demand secure byzantine resilient routing protocol for wireless ad hoc networks," *ACM Trans. Inf. Syst. Secur.*, vol. 10, no. 4, pp. 11–35, 2008.

[6] K. Balakrishnan, J. Deng, and P. K. Varshney, "TWOACK: Preventing selfishness in mobile ad hoc networks," in *Proc. IEEE Wireless Commun. Netw. Conf.*, 2005, pp. 2137–2142.

[7] D. Boneh, B. Lynn, and H. Shacham, "Short signatures from the weil pairing," *J. Cryptol.*, vol. 17, no. 4, pp. 297–319, Sep. 2004.

[8] S. Buchegger and J. Y. L. Boudec, "Performance analysis of the confidant protocol (cooperation of nodes: Fairness in dynamic adhoc networks)," in *Proc. 3rd ACM Int. Symp. Mobile Ad Hoc Netw. Comput. Conf.*, 2002, pp. 226–236.

[9] L. Buttyan and J. P. Hubaux, "Stimulating cooperation in self-organizing mobile ad hoc networks," *ACM/Kluwer Mobile Netw. Appl.*, vol. 8, no. 5, pp. 579–592, Oct. 2003.

[10] J. Crowcroft, R. Gibbens, F. Kelly, and S. Ostring, "Modelling incentives for collaboration in mobile ad hoc networks," presented at the First Workshop Modeling Optimization Mobile, Ad Hoc Wireless Netw., Sophia Antipolis, France, 2003.

[11] J. Eriksson, M. Faloutsos, and S. Krishnamurthy, "Routing amid colluding attackers," in *Proc. IEEE Int. Conf. Netw. Protocols,* 2007, pp. 184–193.

[12] W. Galuba, P. Papadimitratos, M. Poturalski, K. Aberer, Z. Despotovic, and W. Kellerer, "Castor: Scalable secure routing for ad hoc networks," in *Proc. IEEE INFOCOM*, Mar. 2010, pp. 1 –9.

[13] T. Hayajneh, P. Krishnamurthy, D. Tipper, and T. Kim, "Detecting malicious packet dropping in the presence of collisions and channel errors in wireless ad hoc networks," in *Proc. IEEE Int. Conf. Commun.*, 2009, pp. 1062–1067.

[14] Q. He, D. Wu, and P. Khosla, "Sori: A secure and objective reputation-based incentive scheme for ad hoc networks," in *Proc. IEEE Wireless Commun. Netw. Conf.*, 2004, pp. 825–830.

[15] D. B. Johnson, D. A. Maltz, and J. Broch, "DSR: The dynamic source routing protocol for multi-hop wireless ad hoc networks," in *Ad Hoc Networking*. Reading, MA, USA: Addison-Wesley, 2001, ch. 5, pp. 139–172.

[16] W. Kozma Jr. and L. Lazos, "Dealing with liars: Misbehavior identification via Renyi-Ulam games," presented at the Int. ICST Conf. Security Privacy in Commun. Networks, Athens, Greece, 2009.

[17] W. Kozma Jr., and L. Lazos, "REAct: Resource-efficient accountability for node misbehavior in ad hoc networks based on random audits," in *Proc. ACM Conf. Wireless Netw. Secur.*, 2009, pp. 103–110.

[18] K. Liu, J. Deng, P. Varshney, and K. Balakrishnan, "An acknowledgement-based approach for the detection of routing misbehavior in MANETs," *IEEE Trans. Mobile Comput.*, vol. 6, no. 5, pp. 536–550, May 2006.

[19] Y. Liu and Y. R. Yang, "Reputation propagation and agreement in mobile ad-hoc networks," in *Proc. IEEE WCNC Conf.*, 2003, pp. 1510–1515.

[20] S. Marti, T. J. Giuli, K. Lai, and M. Baker, "Mitigating routing misbehavior in mobile ad hoc networks," in *Proc. ACM MobiCom Conf.*, 2000, pp. 255–265.

[21] G. Noubir and G. Lin, "Low-power DoS attacks in data wireles lans and countermeasures," *ACM SIGMOBILE Mobile Comput. Commun. Rev.*, vol. 7, no. 3, pp. 29–30, Jul. 2003.

[22] V. N. Padmanabhan and D. R. Simon, "Secure traceroute to detect faulty or malicious routing," in *Proc. ACM SIGCOMM Conf.*, 2003, pp. 77–82.

[23] P. Papadimitratos and Z. Haas, "Secure message transmission in mobile ad hoc networks," *Ad Hoc Netw.*, vol. 1, no. 1, pp. 193–209, 2003.

[24] A. Proano and L. Lazos, "Selective jamming attacks in wireless networks," in *Proc. IEEE ICC Conf.*, 2010, pp. 1–6.

[25] A. Proano and L. Lazos, "Packet-hiding methods for preventing selective jamming attacks," *IEEE Trans. Depend. Secure Comput.*, vol. 9, no. 1, pp. 101–114, Jan./Feb. 2012.

[26] R. Rao and G. Kesidis, "Detecting malicious packet dropping using statistically regular traffic patterns in multihop wireless networks that are not bandwidth limited," in *Proc. IEEE GLOBECOM Conf.*, 2003, pp. 2957–2961.

[27] H. Shacham and B. Waters, "Compact proofs of retrievability," in *Proc. Int. Conf. Theory Appl. Cryptol. Inf. Secur.*, Dec. 2008, pp. 90–107.

[28] T. Shu, M. Krunz, and S. Liu, "Secure data collection in wireless sensor networks using randomized dispersive routes," *IEEE Trans. Mobile Comput.*, vol. 9, no. 7, pp. 941–954, Jul. 2010.

[29] T. Shu, S. Liu, and M. Krunz, "Secure data collection in wireless sensor networks using randomized dispersive routes," in *Proc. IEEE INFOCOM Conf.*, 2009, pp. 2846–2850.

[30] C. Wang, Q. Wang, K. Ren, and W. Lou, "Privacy-preserving public auditing for data storage security in cloud computing," in *Proc. IEEE INFOCOM Conf.*, Mar. 2010, pp. 1–9.

[31] W. Xu, W. Trappe, Y. Zhang, and T. Wood, "The feasibility of launching and detecting jamming attacks in wireless networks," in *Proc. ACM MobiHoc Conf.*, 2005, pp. 46–57.

[32] Y. Xue and K. Nahrstedt, "Providing fault-tolerant ad-hoc routing service in adversarial environments," *Wireless Pers. Commun., Special Issue Secur. Next Generation Commun.*, vol. 29, no. 3, pp. 367–388, 2004.

[33] Y. Zhang, L. Lazos, and W. Kozma, "AMD: Audit-based misbehavior detection in wireless ad hoc networks," *IEEE Trans. Mobile Comput.*, PrePrint, Vol. 99, published online on 6 Sept. 2013.

[34] S. Zhong, J. Chen, and Y. R. Yang, "Sprite: A simple cheat-proof, credit-based system for mobile ad-hoc networks," in *Proc. IEEE INFOCOM Conf.*, 2003, pp. 1987–1997.

Tao Shu received the BS and MS degrees in electronic engineering from the South China University of Technology, Guangzhou, China, in 1996 and 1999, respectively, and the PhD degree in communication and information systems from Tsinghua University, Beijing, China, in 2003. He received the PhD degree in electrical and computer engineering from the University of Arizona in December 2010. He was a senior engineer at Qualcomm Inc. at San Jose, CA, from December 2010 to July 2011. He is currently an assistant professor at the Department of Computer Science and Engineering, Oakland University. His research aims at addressing the security, privacy, and performance issues in wireless networking systems, with strong emphasis on system architecture, protocol design, and performance modeling and optimization.

Marwan Krunz received the PhD degree in electrical engineering from Michigan State University in 1995. He is a professor of electrical and computer engineering at the University of Arizona. He holds a joint (courtesy) appointment at the same rank at the Department of Computer Science. He is the site co-director of Broadband Wireless Access and Applications Center (BWAC), a recently inaugurated US National Science Foundation (NSF)/industry IUCRC center that includes five universities and 20+ industry members. From 2008 to 2014, he was the UA site director of the NSF IUCRC "Connection One" center. He joined the University of Arizona in January 1997, after a brief postdoctoral stint at the University of Maryland. In 2010, he was a visiting chair of excellence at the University of Carlos III de Madrid, and concurrently a visiting researcher at Institute IMDEA Networks. In 2011, he received the Fulbright Senior Expert Award, through which he visited with the University of Jordan, King Abdullah II School of Information Technology. He previously held other visiting research positions at INRIA-Sophia Antipolis, HP Labs - Palo Alto, University of Paris VI, University of Paris V, and US West Advanced Technologies. His research interests lie in the areas of wireless communications and networking, with emphasis on resource management, adaptive protocols, and security issues. Recently, he has been involved in projects related to cognitive radios and dynamic spectrum access, wireless security, power-controlled protocols for wireless networks, multichannel MIMO systems, secure satellite communications, energy management in solar-powered WSNs, and full-duplex communications. He has published more than 200 journal articles. He received the 2012 IEEE Communications Society TCCC Outstanding Service Award. He received the US NSF CAREER award in 1998. He currently serves on the editorial board for the *IEEE Transactions on Network and Service Management*. Previously, he served on the editorial boards for the *IEEE/ACM Transactions on Networking*, the *IEEE Transactions on Mobile Computing*, the *Computer Communications Journal*, and the *IEEE Communications Interactive Magazine*. He was a guest coeditor for special issues in *IEEE Micro* and *IEEE Communications* Magazines. He was the general cochair for the ACM WiSec 2012 Conference, and served as a TPC chair for various international conferences, including INFOCOM'04, SECON'05, and WoWMoM'06. He has served and continues to serve on the executive and technical program committees of numerous international conferences, and on the panels of several funding agencies. He was the keynote speaker, an invited panelist, and a tutorial presenter at various international conferences. He is a fellow of the IEEE, an Arizona Engineering Faculty Fellow (2011-2014), and an IEEE Communications Society Distinguished lecturer (2013 and 2014).